a

Semileptonic B decays at the B factories

R. Sacco
Department of Physics, Queen Mary, University of London, Mile End Road, London E1 4NS, UK

I present in this review recent results on semileptonic B decays at the B factories.

1 Introduction

Semileptonic B decays to charm and charmless mesons are the primary tool where to measure the CKM matrix elements $|V_{cb}|$ and $|V_{ub}|$ because of their simple theoretical description at the parton level. Their relatively large decay rates are proportional to $|V_{cb}|^2$ and $|V_{ub}|^2$ and depend on the quark masses m_b, m_c. In recent years, tremendous progress has been made in the description of semileptonic and radiative decays in the framework of Heavy Quark Expansions (HQEs); calculations for their width and moments of inclusive observables with restrictions on the phase space are now available in different schemes through order $1/m_b^3$.

2 HQE Parameters Determination

Making use of HQEs it is possible to perform a combined fit to measured moments for which correlation matrices are published. These include moments of the hadronic mass distribution $\langle M_X^n \rangle$ and moments of the lepton energy spectrum $\langle E_\ell^n \rangle$ in inclusive $B \to X_c \ell \bar{\nu}$ as well as moments of the photon energy spectrum $\langle E_\gamma^n \rangle$ in inclusive $B \to X_s \gamma$ decays for different minimum lepton and photon energies. The important issue in this approach is the ability to separate non-perturbative corrections (expressed as a series in powers of $1/m_b$), and perturbative corrections (expressed in powers of α_S). There are various different methods to handle the energy scale μ used to separate long-distance from short-distance physics.

There are two schemes that will be considered in this paper: Kinetic [2] and 1S [1] scheme.

2.1 Experimental Input

Belle has measured the partial branching fractions $\mathcal{B}(B \to X_c \ell \bar{\nu})_{E_\ell > E_{min}}$ and the first, second, third and fourth moments of the truncated electron energy spectrum in $B \to X_c e \bar{\nu}$, $\langle E_\ell \rangle_{E_\ell > E_{min}}$, $\langle (E_\ell - \langle E_\ell \rangle)^2 \rangle_{E_\ell > E_{min}}$, $\langle (E_\ell - \langle E_\ell \rangle)^3 \rangle_{E_\ell > E_{min}}$, $\langle (E_\ell - \langle E_\ell \rangle)^4 \rangle_{E_\ell > E_{min}}$, for nine different electron energy thresholds ($E_{min} = 0.4$, 0.6, 0.8, 1.0, 1.2, 1.4, 1.6, 1.8 and 2.0 GeV) [3]. Belle has also measured the first, second central and second non-central moments of the hadron invariant mass squared (M_X^2) spectrum in $B \to X_c \ell \bar{\nu}$, $\langle M_X^2 \rangle_{E_\ell > E_{min}}$, $\langle (M_X^2 - \langle M_X^2 \rangle)^2 \rangle_{E_\ell > E_{min}}$, and $\langle M_X^4 \rangle_{E_\ell > E_{min}}$ for seven different lepton energy thresholds ($E_{min} = 0.7$, 0.9, 1.1, 1.3, 1.5, 1.7 and 1.9 GeV) [4]. For $B \to X_s \gamma$, Belle has measured the first and second moments of the truncated photon energy spectrum, $\langle E_\gamma \rangle_{E_\gamma > E_{min}}$ and $\langle (E_\gamma - \langle E_\gamma \rangle)^2 \rangle_{E_\gamma > E_{min}}$, for six minimum photon energies ($E_\gamma = 1.8$, 1.9, 2.0, 2.1, 2.2 and 2.3 GeV) [5]. Out of the 71 measurement of inclusive spectra, the ones that have no correspondig theoretical prediction were not used to determine HQE parameters, along with the ones with higher cutoff energies (*i.e.* electron energy and hadron mass moments with $E_{min} > 1.5$ GeV and photon energy moments with $E_{min} > 2$ GeV). Points where correlations with neighbouring points are too high were also excluded.

2.2 Kinetic Scheme

Inclusive spectral moments of $B \to X_c \ell \bar{\nu}$ have been derived in the Kinetic scheme up to $\mathcal{O}(1/m_b^3)$. Theoretical expressions of these moments depend on the b- and c-quark masses $m_b(\mu)$ and $m_c(\mu)$, the non-perturbative parameters $\mu_\pi^2(\mu)$ and $\mu_G^2(\mu)$ ($\mathcal{O}(1/m_b^2)$), $\rho_D^3(\mu)$ and $\rho_{LS}^3(\mu)$ ($\mathcal{O}(1/m_b^3)$), and α_S. A χ^2 function can be written, that combines the measured moments and the corresponding kinetic scheme predictions that depend on these free parameters. A fit that minimizes the χ^2 function and that takes into account both experimental and theoretical uncertainties was performed, where the CKM matrix element $|V_{cb}|$ was treated it as an eighth free parameter. The fit results are summarized in the following [6]:

$$
\begin{aligned}
|V_{cb}| &= (41.93 \pm 0.65_{fit} \pm 0.07_{\alpha_S} \pm 0.63_{th}) \times 10^{-3}, \\
m_B &= 4.564 \pm 0.076_{fit} \pm 0.003_{\alpha_S} \mathrm{GeV}, \\
mc &= 1.105 \pm 0.116_{fit} \pm 0.005_{\alpha_S} \mathrm{GeV}, \\
\mathcal{B}(B \to X_c \ell \bar{\nu}) &= 10.590 \pm 0.164_{fit} \pm 0.006_{\alpha_S} \%,
\end{aligned}
$$

where first error is due to all uncertainties taken into account in the fit (experimental error in the moment measurements, non-perturbative corrections and bias correction to the moments, uncertainty in τ_B), the second error comes from the uncertainty in α_S, and the last error in the expression of $|V_{cb}|$ is a 1.5% uncertainty due to the limited accuracy of the theoretical expression for the semileptonic width. The fit results for m_b, μ_π^2 and ρ_D^3 are shown in Figure 1.

2.3 1S scheme

The inclusive spectral moments of $B \to X_c \ell \bar{\nu}$ have also been derived in the 1S scheme up to $\mathcal{O}(\infty/\Updownarrow_\lfloor^\ni)$. A total of seven parameters were determined: $|V_{cb}|$, Λ, λ_1, τ_1, τ_2, τ_3 and ρ_1. The parameter Λ is the difference between the b-quark mass and the reference value about which it is expanded, *i.e.*, $\Lambda = m_{\Upsilon(1S)}/2 - m_b^{1S}$, and results will be quoted in terms of m_b^{1S}. A fit to a χ^2 function that combines the measured moments and the corresponding 1S scheme predictions and that takes into account both experimental and theoretical uncertainties was performed, giving the results [6]:

$$
\begin{aligned}
|V_{cb}| &= (41.49 \pm 0.52_{fit} \pm 0.20_{\tau_B}) \times 10^{-3}, \\
m_b^{1S} &= (4.729 \pm 0.048)\ \mathrm{GeV}, \\
\lambda_1 &= (0.30 \pm 0.04)\ \mathrm{GeV}^2,
\end{aligned}
$$

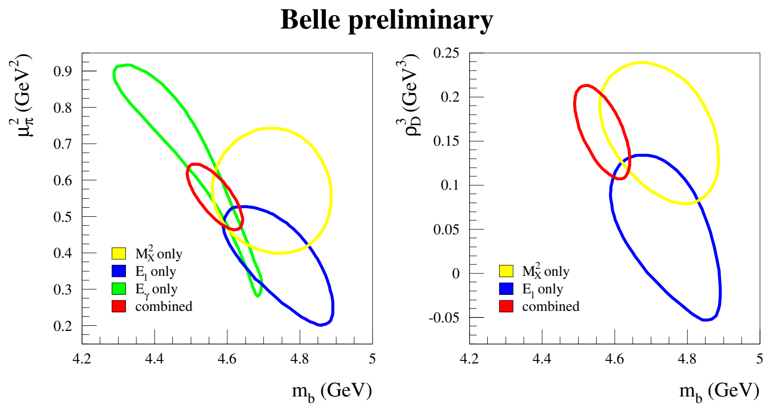

Figure 1: Fit results for m_b and μ_π^2 (left) and m_b and ρ_D^3 in the Kinetic Scheme. The fit is done using lepton energy moments only (blue), hadron mass moments only (yellow), photon energy moments (green) only and all moments combined (red). The ellipses correspond to $\Delta\chi^2 = 1$.

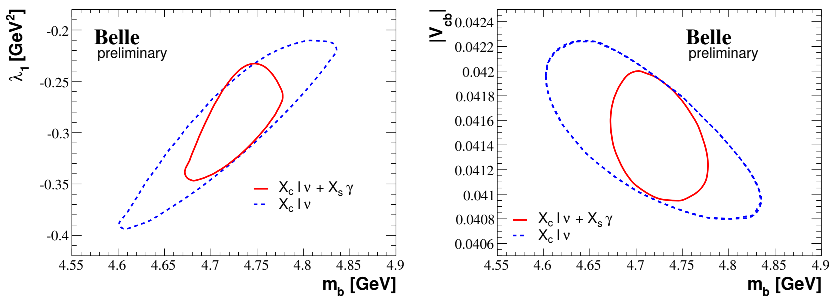

Figure 2: Fit results for m_b^{1S} and λ_1 (left) and m_b^{1S} and $|V_{cb}|$ (right) in the 1S Scheme. The fit to the $B \to X_c \ell \bar{\nu}$ data only ($B \to X_c \ell \bar{\nu}$ and $B \to X_s \gamma$ data combined) is shown by a dashed blue line (solid red line). The regions correspond to $\Delta\chi^2 = 1$.

where the first error is the uncertainty from the fit including experimental and theory errors, and the second error (on $|V_{cb}|$ only) is due to the uncertainty on the average B lifetime. The fit results for m_b^{1S}, λ_1 and $|V_{cb}|$ are shown in Figure 2.

3 Relative Branching Fractions for $B \to D, D^*, D^{**} \ell \nu$ Decays

The determination of the exclusive branching fractions of $B \to X_c \ell \bar{\nu}$ decays is an essential part of the program of studies of semileptonic B meson decays at the B-factories to understand the dynamics of semileptonic decays of the b quark and determine the relevant CKM matrix elements. The mass of the hadronic system X_c, recoiling against the fermionic pair in the decay, is a crucial parameter both in the extraction of $|V_{cb}|$, in exclusive semileptonic decays, and in isolating $B \to X_u \ell \bar{\nu}$ decays for determining $|V_{ub}|$. It is also important in the measurement of the heavy quark masses and other non-perturbative OPE parameters from the distribution of spectral moments in semileptonic decays.

BABAR has presented a novel technique[7] to extract the exclusive relative branching fractions for $B \to D \ell \bar{\nu}$, $B \to D^* \ell \bar{\nu}$ and $B \to D^{**} \ell \bar{\nu}$ with $\ell = e, \mu$ in an inclusive sample of $B \to D X \ell \bar{\nu}$ events, where X can be either nothing or any particle(s) from a semileptonic B decay into a higher mass charm state, or a non-resonant state. D^{**} is a hadronic final state containing a charm meson, with a total mass above the D^* mass, therefore including both D^{**} mesons and non-resonant $D^{(*)} + n\pi$ states.

The analysis is based on 339.4 fb^{-1} of data collected at the $\Upsilon(4S)$ resonance with the *BABAR*

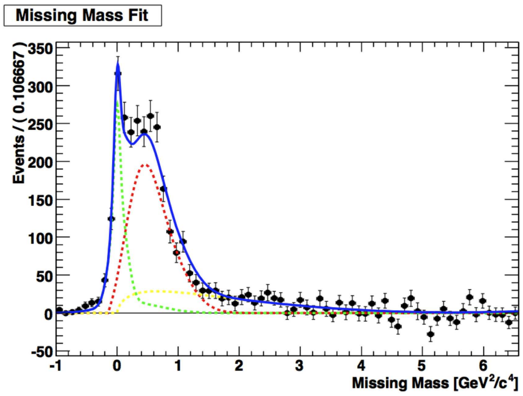

Figure 3: Fitted $m^2_{miss,D}$ distribution for $B^0 \to DX\ell\bar{\nu}$.

Table 1: Fitted ratios of branching fractions with statistical and systematic uncertainties

Ratio	B^- (%)	B^0 (%)
$\frac{\Gamma(B\to D\ell\bar{\nu})}{\Gamma(B\to DX\ell\bar{\nu})}$	$22.7 \pm 1.4 \pm 1.6$	$21.5 \pm 1.6 \pm 1.3$
$\frac{\Gamma(B\to D^*\ell\bar{\nu})}{\Gamma(B\to DX\ell\bar{\nu})}$	$58.2 \pm 1.8 \pm 3.0$	$53.7 \pm 3.1 \pm 3.6$
$\frac{\Gamma(B\to D^{**}\ell\bar{\nu})}{\Gamma(B\to DX\ell\bar{\nu})}$	$19.1 \pm 1.3 \pm 1.9$	$24.8 \pm 3.2 \pm 3.0$

detector at the PEP-II asymmetric-energy e^+e^- storage rings. Signal B mesons are selected by fully reconstructing the accompanying B meson (B_{tag}), which allows to constrain the kinematics, to reduce the combinatorial background and to determine the charge of the signal B.

A set of three largely uncorrelated variables to discriminate between the different semileptonic decay modes in the reconstructed $B \to DX\ell\bar{\nu}$ sample was chosen. These are: the lepton momentum in the center-of-mass frame, $|\vec{p}_\ell|$; the missing mass squared reconstructed with respect to the $D\ell$ system, which corresponds to the mass of the $X\bar{\nu}$ system, $m^2_{miss,D} = (p_\Upsilon - p_{B_{tag}} - p_D - p_\ell)^2$; the number of reconstructed charged tracks in addition to those used for reconstructing the $D\ell$ system and the B_{tag}, N_{trks}. In order to reduce the sensitivity to the modeling of the decays to the different charm states, the shapes of these variables were extracted from the data itself, using samples highly enriched in the relevant decay modes. The relative D, D^*, D^{**} contributions were then determined by a multi-parameter fit to the inclusive sample. The result of the fit to the missing mass distribution for $B^0 \to DX\ell\bar{\nu}$ is shown in Figure 3. The relative branching fractions for $B^- \to D^0, D^{*0}, D^{**0}\ell\bar{\nu}$ and $B^0 \to D^+, D^{*+}, D^{**+}\ell\bar{\nu}$, with statistical and systematic uncertainties are given in Table 1.

4 Simultaneous Determination of the $B^0 \to D^{*-}\ell^+\nu_e$ Form Factors and of $|V_{cb}|$

In the Standard Model, the rate of the $B^0 \to D^{*-}\ell^+\nu_e$ decay is proportional to $|V_{cb}|^2$. The decay is also influenced by strong interactions, parameterized by two axial form factors A_1 and A_2, and one vector form factor V, each of which depends on the momentum transfer squared q^2 of the B meson to the D^* meson. The form of this dependence is not known *a priori*. In the framework of heavy-quark effective field theory (HQET) [8,9], these three form factors are related to each other through heavy quark symmetry (HQS), but HQET leaves three free parameters, which must be determined by experiment. The form factors are usually characterized in terms of their ratio parameters R_1 and R_2, and a slope parameter ρ^2.

The extraction of $|V_{cb}|$ relies on the measurement of differential decay rates. HQS predicts the normalization of the decay rate at the maximum q^2, and $|V_{cb}|$ is determined from an extrapolation of the form factors to this value. The precise determination requires corrections to the HQS prediction for the normalization as well as a measurement of the variation of the form factors near the maximum q^2, where the decay rate goes to zero as the phase space vanishes.

79 fb^{-1} of $B\overline{B}$ events collected with the *BABAR* detector were analyzed [10]; in place of a linear parameterization of the q^2 dependence of the form factors, a higher-order polynomial was used. The Lorentz structure of the $B \to D^* \ell \nu$ decay amplitude can be expressed in terms of three helicity amplitudes which correspond to the three polarization states of the D^*. The full differential decay rate can be expressed in terms of four kinematic variables: the Lorentz-invariant w (the dot product of the B and D^* four-velocities) and three angles θ_ℓ (the angle between the direction of the lepton in the virtual W rest frame, and the direction of the virtual W in the B rest frame), θ_V (the angle between the direction of the D in the D^* rest frame) and χ (the dihedral angle between the plane formed by the $D^* - D$ and the plane formed by the $W - \ell$ system).

$|V_{cb}|$ and the form factors were extracted by performing a χ^2 fit of three one-dimensional distributions, as it was found that the χ distribution is insensitive to the form factor parameters. The three other kinematic variables were divided into ten bins, and a least-square fit of the projected one-dimensional distributions was performed, correcting for background contributions. The result of the fit is shown in Figure 4.

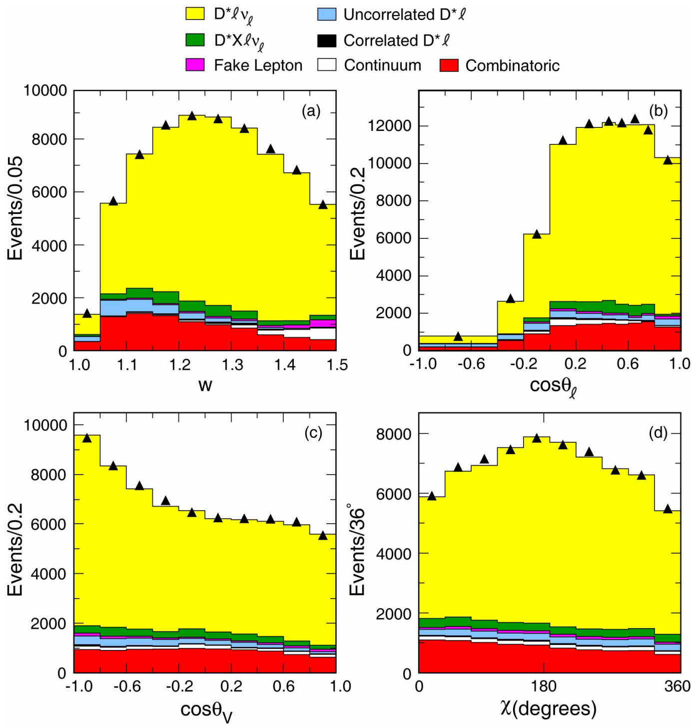

Figure 4: Comparison of the measured distributions (data points) a) w, b) $\cos\theta_\ell$, c) $\cos\theta_V$, and d) χ, with the result of the fit, shown as the sum of the fitted signal yield and the estimated background distributions. The statistical uncertainties of the data are too small to be visible.

The results of the extraction of $|V_{cb}|$ and the form factors were then combined with the results of an earlier *BABAR* measurement [11], based on an unbinned maximum-likelihood fit to the four-dimensional decay distribution; this fit is sensitive to the interference of the three helicity amplitudes and thus results in significant smaller uncertainties on the form-factor parameters.

Table 2: Partial branching fractions in three bins of q^2. These are summed to give the full branching fraction quoted in the Sum column. Errors are statistical and systematic.

Mode	$\Delta\mathcal{B}$ (10^{-4}) $0 < q^2 < 8$ (GeV^2/c^2)	$8 < q^2 < 16$ (GeV^2/c^2)	$q^2 > 16$ (GeV^2/c^2)	$\mathcal{B}$ (10^{-4}) Sum (GeV^2/c^2)
$B \to \pi^+\ell\nu$	$0.50 \pm 0.14 \pm 0.02$	$0.68 \pm 0.18 \pm 0.03$	$0.31 \pm 0.12 \pm 0.01$	$1.49 \pm 0.26 \pm 0.06$
$B \to \pi^0\ell\nu$	$0.28 \pm 0.09 \pm 0.02$	$0.22 \pm 0.08 \pm 0.04$	$0.36 \pm 0.12 \pm 0.02$	$0.86 \pm 0.17 \pm 0.06$

Taking into account the correlation between the two measurements, *BABAR* obtains:

$$\begin{aligned}
\mathcal{F}(1)|V_{cb}| &= (34.7 \pm 0.3 \pm 1.1) \times 10^{-3} \\
\rho^2 &= 1.179 \pm 0.048 \pm 0.028 \\
R_1(1) &= 1.417 \pm 0.061 \pm 0.044 \\
R_2(1) &= 0.836 \pm 0.037 \pm 0.022.
\end{aligned}$$

5 Branching Fractions for Exclusive $B \to X_u \ell \bar{\nu}$ Decays

Exclusive charmless semileptonic decays can be used to extract the CKM matrix element $|V_{ub}|$. It is the aim of an ongoing programme of measurements at the B factories to improve the determination of $|V_{ub}|$ with a precision better than 5%, for comparison with the inclusive results, which have somewhat different experimental and theoretical uncertainties.

The Belle collaboration has recently presented studies of the exclusive semileptonic decays $B \to \pi^+\ell\nu$, $B \to \pi^0\ell\nu$, $B \to \rho^+\ell\nu$, $B \to \rho^0\ell\nu$ and $B \to \omega\ell\nu$ using a full reconstruction tagging technique to identify candidate B mesons [12]. The measurement presented here is based on a data sample that contains 535×10^6 $B\overline{B}$ pairs, collected with the Belle detector at the KEKB asymmetric-energy e^+e^- (3.5 on 8 GeV) collider. One of the two B mesons from the pair is fully reconstructed in hadronic modes, allowing to constrain the kinematics, to reduce the combinatorial background and to determine the charge of the signal B. Signal events are identified by examining the missing mass squared (m^2_{miss}) distributions. If the tagging B is correctly reconstructed and the correct lepton and hadron candidate have been identified on the recoil side, then (ideally) all missing 4-momentum is due to the remaining unidentified neutrino. The square of the missing 4-momentum for signal events should therefore be close to zero, and applying this requirement provides a very strong discrimination between signal and background. Fitting the m^2_{miss} distributions, it is possible to identify signal and background components. The fitted number of signal was: 48 ± 8 for $B \to \pi^+\ell\nu$, 35 ± 7 for $B \to \pi^0\ell\nu$, 41 ± 9 for $B \to \rho^+\ell\nu$, 61 ± 9 for $B \to \rho^0\ell\nu$ and 27 ± 9 $B \to \omega\ell\nu$. Partial branching fractions were extracted in bins of q^2, the invariant mass squared of the lepton-neutrino system, in order to minimize the systematic error which arises from the lack of precise knowledge of the shape of the form factors. Three bins in q^2 were chosen, 0 to 8 GeV^2/c^2, 8 to 16 GeV^2/c^2, and greater than 16 GeV^2/c^2. The results are summarized in table 2.

6 Extraction of $|V_{ub}|$ with Reduced Model Dependence

Theoretically, the most precise predictions can be made for the total $B \to X_u \ell \bar{\nu}$ decay rate. Accounting for restriction in phase space is difficult because decay spectra close to the kinematic limit are susceptible to non-perturbative strong-interaction effects. Theoretical tools for the calculations of the partial inclusive decay rates are QCD factorization and local operator product expansions (OPE). These calculations separate non-perturbative from perturbative quantities, and use expansions in inverse powers of the b-quark mass, and in powers of α_S. Non-perturbative bound-state effects are accounted for by a shape function describing the Fermi-motion of the b quark inside the B meson. These shape functions cannot be calculated. Different shapes have been proposed, and parameters defining these shapes have to be extracted from data. This introduces significant additional hadronic uncertainties. At leading order, these shape functions are assumed to be universal functions for $b \to q$ transitions, where q is a light quark, either s or u. Usually, the non-perturbative parameters of these shape functions, the b-quark mass m_b and its mean kinetic energy squared, $\mu_\pi^2(\mu)$, are extracted from the inclusive photon spectrum in $B \to X_s\gamma$ decays. These parameters depend on the choice of the renormalization scale, μ. It was suggested that $|V_{ub}|$ can be extracted with smaller theoretical uncertainties by combining integrals over the lepton-endpoint spectrum in $B \to X_u\ell\bar{\nu}$ decays with weighted integrals over the photon-endpoint spectrum from $B \to X_s\gamma$ decays. The underlying assumption is that the QCD interactions affecting these two processes are the same and thus will cancel to first order in the appropriate ratio of weighted rates. The advantage of this approach is that it reduces the sensitivity to the choice of the shape-function parameterization and thus avoids uncertainties that are difficult to quantify.

BABAR has presented the extraction of $|V_{ub}|$ [16] based on different prescriptions proposed by Leibovich, Low, and Rothstein (LLR) [13], by Neubert [14], and more recent calculations by Lange, Neubert, and Paz (LNP) [15].

The experimental inputs for this analysis are the published *BABAR* measurements of the inclusive electron energy spectrum in $B \to X_u\ell\bar{\nu}$ decays [17], and of the inclusive photon-energy spectrum in $B \to X_s\gamma$ decays[18]. These measurements are based on a data sample corresponding to a total integrated luminosity of about 80 fb^{-1}. The measured spectra were integrated above an energy E_0, measured in the B-meson rest frame.

A comparison of the extraction of $|V_{ub}|$ for the three methods considered, with its dependence on the lepton energy cut-off, is shown in Figure 5. The LNP method is more accurate, in the sense that it includes two-loop calculations, and this explains the error inflation that we notice at large lepton energy cut-off. The three methods agree well at low lepton energy cut-off and give results with a precision comparable to Shape Function based analyses. At present, for $E_0 = 2.0$ GeV, the experimental errors on both the $B \to X_u\ell\bar{\nu}$ branching fraction and the integral over $B \to X_s\gamma$ are about 12%; this means that there are opportunities to improve the accuracy of $|V_{ub}|$ significantly by reducing the experimental errors of these two spectra with more data available now and in the future. Also, extending E_0 to 1.9 GeV or lower, would allow to establish more clearly the stability of the results in this region.

7 Conclusions

The B factories are doing an excellent job of overconstraining the Unitarity Triangle. The extraction of $|V_{cb}|$ from fits to moments in inclusive $B \to X_c\ell\bar{\nu}$ decays has reached a better than 2% precision. $|V_{cb}|$ from exclusive decays is now known with a 5% uncertainty.

On the extraction on $|V_{ub}|$, there are encouraging results from Belle, that has calculated branching fractions from exclusive $B \to X_u\ell\bar{\nu}$. There are also recent theoretical developments that can allow the extraction of $|V_{ub}|$ with a reduced model dependence, exploiting the increasing dataset collected at the B factories.

Finally, the measurement of relative branching fractions for $B \to D, D^*, D^{**}\ell\nu$ decays and of the form factors in $B^0 \to D^{*-}\ell^+\nu_e$ decays has improved our modeling of the hadronic system X_c, crucial in the extraction of $|V_{cb}|$ and in isolating $B \to X_u\ell\bar{\nu}$ decays for determining $|V_{ub}|$.

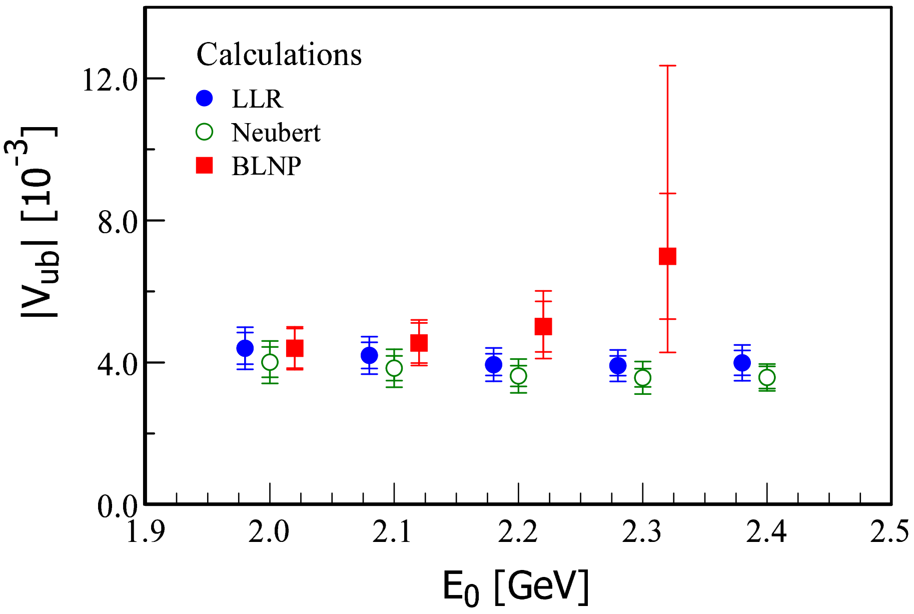

Figure 5: Comparison of $|V_{ub}|$ values extracted from the three different calculations as a function of the lepton energy cut-off, E_0.

References

1. C.W. Bauer, Z. Ligeti, M. Luke and A.V. Manohar, PRD **67**, 050412 (2003); C.W. Bauer, Z. Ligeti, M. Luke, A.V. Manohar and M. Trott, PRD **70**, 094017 (2004);
2. P. Gambino and N. Uraltsev, *Eur. Phys. J.* C **34**, 181 (2004).
3. P. Urquijo, E. Barberio, *et al.* (Belle Collaboration), PRD **75**, 032001 (2007).
4. C. Schwanda, *et al.* (Belle Collaboration), PRD **75**, 032005 (2007).
5. K. Abe *et al.* (Belle Collaboration), hep-ex/0508005.
6. K. Abe *et al.* (Belle Collaboration), hep-ex/0611047.
7. B. Aubert *et al.* (*BABAR* Collaboration), hep-ex/0703027.
8. M. Neubert, Physics Reports, 259 (1994).
9. J.D. Richman and P.R. Burchat, Rev. Mod. Phys. **67**, 893 (1985).
10. B. Aubert *et al.* (*BABAR* Collaboration), hep-ex/0607076.
11. B. Aubert *et al.* (*BABAR* Collaboration), PRD **74**, 092004 (2006).
12. K. Abe *et al.* (Belle Collaboration), hep-ex/0610054.
13. A.K. Leibovich, I. Low, and I.Z. Rothstein, PRD **61**, 053006 (2000); A.K. Leibovich, I. Low, and I.Z. Rothstein, PLB **513**, 83 (2001); I.Z. Rothstein, hep-ph/0111337.
14. M. Neubert, PLB **513**, 88 (2001);
15. B.O. Lange, M. Neubert, and G. Paz, JHEP 0510, 084 (2005).
16. V. Golubev, Y.I. Skovpen, V.G. Lüth, hep-ph/0702072.
17. B. Aubert *et al.* (*BABAR* Collaboration), PRD **73**, 012006 (2006).
18. B. Aubert *et al.* (*BABAR* Collaboration), PRD **72**, 052004 (2005).